Ferroelectric, pyroelectric, and piezoelectric properties of a photovoltaic perovskite oxide

Yang Bai,[a] Tuomo Siponkoski, Jani Peräntie, Heli Jantunen, and Jari Juuti
Microelectronics Research Unit, Faculty of Information Technology and Electrical Engineering, University of Oulu, FI-90014 Oulu, Finland

(Received 4 November 2016; accepted 10 January 2017; published online 7 February 2017)

A perovskite solid-solution, (1-x)$KNbO_3$-x$BaNi_{1/2}Nb_{1/2}O_{3-\delta}$ (KBNNO), has been found to exhibit tunable bandgaps in the visible light energy range, making it suitable for light absorption and conversion applications, e.g., solar energy harvesting and light sensing. Such a common ABO_3–type perovskite structure, most widely used for ferroelectrics and piezoelectrics, enables the same solid-solution material to be used for the simultaneous harvesting or sensing of solar, kinetic, and thermal energies. In this letter, the ferroelectric, pyroelectric, and piezoelectric properties of KBNNO with $x = 0.1$ have been reported above room temperature. The investigation has also identified the optimal bandgap for visible light absorption. The stoichiometric composition and also a composition with potassium deficiency have been investigated, where the latter has shown more balanced properties. As a result, a remanent polarization of 3.4 $\mu C/cm^2$, a pyroelectric coefficient of 26 $\mu C/m^2$ K, piezoelectric coefficients $d_{33} \approx 23$ pC/N and $g_{33} \approx 4.1 \times 10^{-3}$ Vm/N, and a direct bandgap of 1.48 eV have been measured for the KBNNO ceramics. These results are considered to be a significant improvement compared to those of other compositions (e.g., ZnO and AlN), which could be used for the same applications. The results pave the way for the development of hybrid energy harvesters/sensors, which can convert multiple energy sources into electrical energy simultaneously in the same material. *Published by AIP Publishing.* [http://dx.doi.org/10.1063/1.4974735]

Hybrid energy harvesters have been developed in order to convert different energy sources into electricity simultaneously.[1–4] However, these harvesters usually utilize different materials for different harvesting principles or energy sources. In such cases, for a defined space, one has to compromise either on the number of harvested energy sources or on the space taken by different energy harvesting components. One solution to this problem is to design or discover a single composition/material from which multiple energy sources/signals can be harvested/detected simultaneously. A perovskite solid-solution, KBNNO, has recently been reported for its broadly tunable direct bandgap of 1.1–3.8 eV, where the ideal bandgap value for visible light absorption (1.39 eV) is reached with $x = 0.1$.[5] This type of perovskite ferroelectric solid-solution could show a strong piezoelectric and/or pyroelectric response together with a considerable photovoltaic effect, thus providing a unique opportunity to develop a novel multi-source energy harvester or multi-functional sensor based on a single material.

Bulk ceramics of KBNNO with $x = 0.1$ (0.1KBNNO) were fabricated via a mixed oxide solid-state synthesis route. Two different sub-compositions (compositions I and II) were fabricated. The stoichiometry of composition I was strictly in accordance with the chemical formula 0.9$KNbO_3$-0.1$BaNi_{1/2}Nb_{1/2}O_{3-\delta}$, equivalent to $(K_{0.9}Ba_{0.1})(Nb_{0.95}Ni_{0.05})O_{3-0.025}$. In composition II, K^+ was about 11.1 mol. % less compared to that in composition I, resulting in a chemical formula of $(K_{0.8}Ba_{0.1})(Nb_{0.95}Ni_{0.05})O_{3-0.075}$. As the theoretical value of oxygen deficiency (δ) of the doping composition $BaNi_{1/2}Nb_{1/2}O_{3-\delta}$ is 0.25,[5] the designed oxygen vacancy concentrations −0.025 and 0.075 per 3 oxygen atoms (equal to 0.8 mol. % and 2.5 mol. %) in compositions I and II, respectively, were calculated by maintaining the overall chemical valence to be zero after appropriate amounts of all dopants were placed in the matrix ($KNbO_3$). The concentrations of oxygen vacancies were mainly controlled by applying the appropriate amount of doping through accurate weighing using a precise balance with 0.01 mg readability and 1 mg accuracy (ES 225SM-DR, Precisa, Dietikon, Switzerland). Starting compositions of K_2CO_3 (≥99%, J. T. Baker), $BaCO_3$ (99.98%, Aldrich Chemistry), NiO (99.999%, Aldrich Chemistry), and Nb_2O_5 (99.9%, Aldrich Chemistry) were first dried at 220 °C, weighed, and then mixed and milled using a planetary ball mill for 24 h in ethanol and with zirconia balls (3 mm diameter). The dried mixture was calcined at 850 °C for 4 h in air and was milled again with the same procedure. The 8.8 wt. % binder (3.3 wt. % PVA (polyvinyl alcohol) dissolved in deionized water) was subsequently added into the dried calcined powder using manual granulation in a mortar. Pellets were shaped under 62 MPa at room temperature (RT) through uniaxial pressing. The green bodies were sintered at 1150 °C (composition I) and 1125 °C (composition II) for 2 h on Pt foil. They were buried by sacrificial powder of the same composition in a covered alumina crucible in order to inhibit the volatilization of potassium. The calcined powder and bare ceramic samples were characterized under an x-ray diffraction system (XRD, D8 Discover, Bruker, Karlsruhe, Germany) and a scanning electron microscope (SEM, Ultra Plus, ZEISS, Jena, Germany) for microstructural analysis. The theoretical densities were calculated to be in the ranges of 4.7–4.9 g/cm^3 and 4.6–4.8 g/cm^3 for compositions I and II, respectively.[5,6]

[a]Author to whom correspondence should be addressed. Electronic mail: yang.bai@oulu.fi

Approximately 95% theoretical densities were reached by both batches of samples. The polished ceramics were also measured with a UV-Vis-NIR spectrophotometer (Cary 500 Scan, Varian, Palo Alto, USA) for bandgap calculation. The samples with electrodes (Ag paste, DT 1402, Heraeus, fired at 600 °C for 20 min) were measured with a ferroelectric test system (Precision LCII, Radiant Technologies, Inc., Albuquerque, USA) for ferroelectric loops, resistivity, and leakage currents. Finally, the samples with electrodes were poled in silicone oil at 150 °C, which was decreased during poling to about 25 °C while an electric field of 60 kV/cm was maintained. Prior to poling, the domain walls were relaxed by applying 1 Hz AC field of ±80 kV/cm for 100 cycles. The poled samples were tested using a temperature controlled stage (LTS 350, Linkam Scientific Instruments, Tadworth, UK) and an electrometer (B2985A, Keysight, Santa Rosa, USA) to obtain pyroelectric data and using a laser interferometry system (OFV, Polytech, Waldbronn, Germany) to determine the converse piezoelectric coefficient.

Figure 1(a) shows the XRD patterns of powder and sintered ceramics of the composition I and II samples. All powder and ceramic samples formed dominant perovskite microstructures. The patterns of the composition I samples showed a good consistency with previously reported results,[5] where a very weakly tetragonal (close to cubic[7]) ferroelectric phase was identified with the help of the insets of peaks

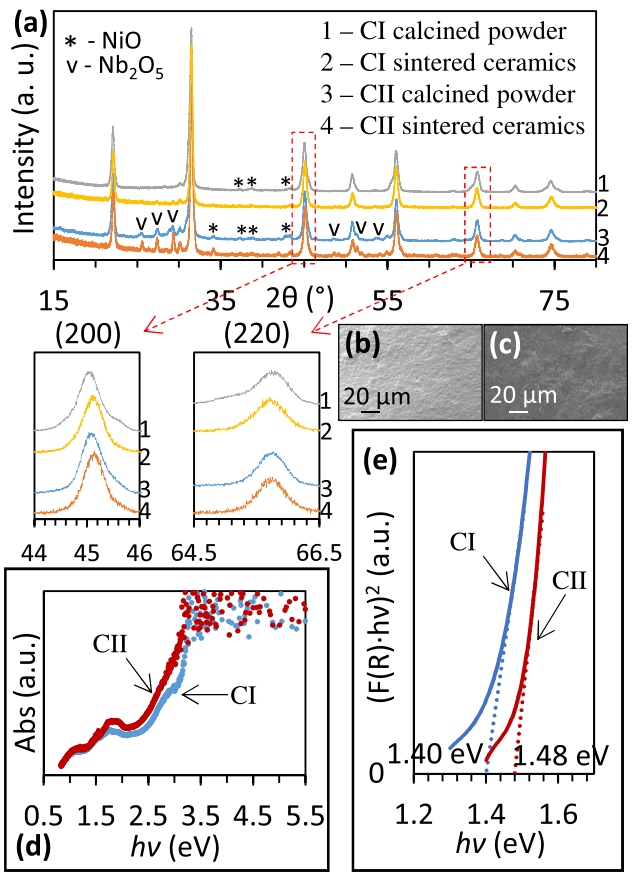

FIG. 1. (a) XRD patterns of the calcined powder and sintered ceramics of compositions I and II; SEM images of sintered ceramics of (b) composition I and (c) composition II; and dependence of (d) Absorbance (Abs) and (e) $(F(R)\cdot h\nu)^2$ on $h\nu$ for the sintered ceramics of compositions I and II. Compositions I and II are abbreviated as CI and CII, respectively.

(200) and (220), which were slightly broadened towards lower angles. Minor NiO was found in composition I, which is also consistent with the reference.[5] More obviously, excessive Nb_2O_5 (monolithic) and NiO, which did not form into a solid-solution, were observed in the patterns of composition II samples. This resulted from the off-stoichiometric K^+, leading to excessive Nb^{5+} and Ni^{2+}. As potassium volatiles above 800 °C,[8] the composition II sintered ceramics showed more Nb_2O_5 than their powder counterpart, implying further loss of potassium during sintering. Despite the excessive Nb_2O_5 and NiO, composition II samples showed similar patterns to composition I. The existence of oxygen vacancies can be confirmed in both compositions because all the sintered samples were non-conductive, whereas a fully oxidized KBNNO composition with $\delta = 0$ was predicted to be in the metallic state.[5] Also, the formation of oxygen vacancies has been considered to be favorable in the compositions and under the synthesis conditions according to free-energy calculations.[5,9] The presence of oxygen vacancies, resulting ultimately in the suppression of domain wall movement (domain wall pinning effect) caused by defect dipoles of acceptor ions and oxygen vacancy, is widely known. This will lower dielectric permittivity and loss, resistivity, and piezoelectric properties whilst increasing the mechanical quality factor and coercive electric field.[10,11] Such a situation is not ideal in terms of applications in energy harvesting or sensing through piezoelectric and/or pyroelectric effects where stronger piezoelectricity and domain wall mobility are preferred. However, the combinations of Ni^{2+} ion and oxygen vacancy were compulsory for this investigation because they usefully elevate electronic states in the gap of KN—the parent composition. Figures 1(b) and 1(c) show the SEM images of fracture surfaces of the sintered ceramics of compositions I and II, respectively, showing dense structures with only a few pores recognized. Figure 1(d) shows the optical absorption spectra of composition I and II ceramic samples. Although it gives the general information that the bandgaps were in the range of 1–1.5 eV, it is still open to question whether this method is sufficiently reliable to define the bandgaps of disordered compositions. The presented compositions are not fully disordered, but the oxygen vacancies would contribute to disorder to some extent, with evidence of a "tail" in the optical absorption spectrum of each composition that expands deeply into the forbidden band.[12] It might be possible that the defects in the unit cells acted as a barrier and participated in the interaction with photons.[12] Therefore, a more reliable method, presented below (Figure 1(e)), was used to determine the bandgaps. Figure 1(e) plots $(F(R)\cdot h\nu)^2$ as a function of $h\nu$ for the sintered ceramics of compositions I and II, where h is Planck's constant and ν is the light frequency. F(R) is a function of the reflectance (R) and was directly measured with the spectrophotometer. Theoretically, $F(R) = (1-R)^2/2R$, which has been used as a reliable factor and simple method to determine the bandgaps of solid materials.[13] The composition I samples exhibited a bandgap of 1.40 eV, showing a considerable consistency with the reference.[5] The composition II samples had a bandgap of 1.48 eV, which is slightly larger than that of composition I but is still smaller than the lowest photon energy (1.65 eV) of the visible light spectrum.[5] The

increased bandgap of composition II might be because of fewer "effective" combinations of Ni^{2+} and oxygen vacancies in the unit cells,[5] which were compensated by K^+ vacancies introduced at the same time to the composition. This phenomenon is essential as K^+ vacancies together with oxygen vacancies started to show a complex and comprehensive effect on the photovoltaic properties and were also likely to have an effect on the ferroelectric properties (as shown in Figure 2).

Figure 2(a) shows the hysteresis loops measured with 1 Hz frequency with a maximum electric field of 80 kV/cm at room temperature (RT) and 150 °C, respectively. At RT, a loop with the thin and elongated shape was observed, where the maximum polarization at 80 kV/cm field reached approximately 8 $\mu C/cm^2$, while the corresponding remanent polarization was only about 1 $\mu C/cm^2$. The remanent polarization was consistent with that reported previously.[5] The maximum and remanent polarizations were both significantly reduced from values of $>20\ \mu C/cm^2$ and $10\ \mu C/cm^2$, respectively, obtained for pure KN ceramics at the same temperature and with the same applied field.[14] This was either due to the reduced asymmetry of the unit cell[5,7] or because the loop was only partially saturated. Constricted loops caused by the domain wall pinning effect are well known in ferroelectrics with oxygen vacancies.[15] It is also known that elevated temperature, increased number of applied electric field cycles, and reduced electric field frequency may help to reduce the pinning effect.[16,17] In order to estimate the full remanent polarization, all of the above methods were employed. At an elevated temperature of 150 °C (Figure 2(a)), more effective domain switching, compared to that at RT, resulted in an increased remanent polarization of approximately 2.5 $\mu C/cm^2$. A similar trend could be observed for the parental composition, KN, where the remanent polarization was increased to approximately $20\ \mu C/cm^2$ at 110 °C.[14] Figure 2(b) shows the remanent polarization, coercive field, resistivity, and leakage current measured with the hysteresis loops at different temperatures. A substantial increase in the remanent polarization with temperature was observed between 100 and 150 °C, whilst a corresponding dramatic decrease in resistivity was realized in the same range. Although the decreased resistivity led to increased leakage current, there was no evidence that it would lead to ineffective poling. In contrast, a strong negative correlation between remanent polarization and temperature was reported in the range of −200 °C to RT.[5] The trend observed above RT may be because of a phase transition around 170 °C,[5] thus making domain reorientation more active at 150 °C. After the first hysteresis loop measurement, 100 consecutive cycles of AC field (standard bipolar signal) with an amplitude of 80 kV/cm were applied to the samples, at both RT and 150 °C. Figure 2(c) shows the variation of the maximum and remanent

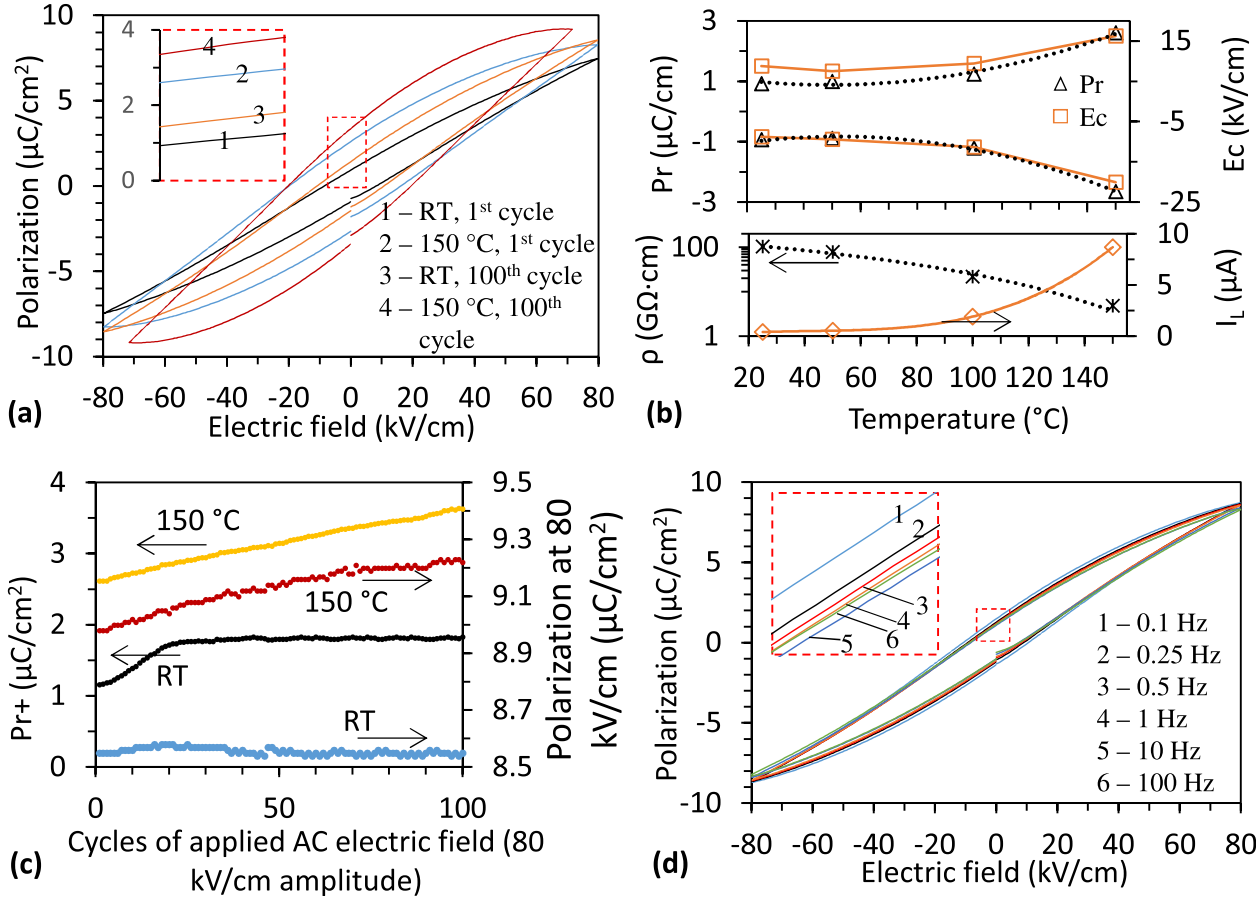

FIG. 2. (a) Ferroelectric hysteresis loops measured at room temperature (RT) and 150 °C and at the 1st and 100th applied field cycles, respectively; (b) Dependence of remanent polarization (Pr; positive and negative), coercive electric field (Ec; positive and negative), resistivity (ρ), and leakage current (I_L) on temperature; (c) Dependence of positive remanent polarization (Pr+) and polarization at 80 kV/cm on the number of cycles of applied AC field (domain wall relaxation); and (d) Ferroelectric hysteresis loops measured with different electric field frequencies.

polarizations with the number of cycles. At RT, the maximum polarization almost stayed at the same level, while the remanent polarization experienced a sharp increase by about 50% in the first 25 cycles and then remained the same afterwards. At 150 °C, both the maximum and remanent polarizations increased smoothly and continuously by about 3% and 40%, respectively, in the 100 cycles. Such a phenomenon was expected as the increased numbers of poling cycles tended to compensate the defect charges accumulated in the domain wall regions, thus relaxing the internal stress caused by domain wall pinning.[18] Figure 2(a) also shows the hysteresis loops measured at the 100th applied field cycle at RT and 150 °C, respectively. As a result of domain wall relaxation, the loops at both temperatures became correspondingly wider. Figure 2(d) shows the ferroelectric hysteresis loop measurements at RT and with different electric field frequencies. From 100 Hz down to 0.5 Hz, the changes in the maximum and remanent polarizations could hardly be seen, while increased gaps were found from 0.5 Hz to 0.1 Hz. In these cases, the external electric field was closer to a DC field, and thus, there was more time to compensate the internal defect charges and reduce the pinning effect. It was also found that there was a linear relationship between the remanent polarization and the common logarithm of the frequency for both compositions I and II, as well as for a $Pb(Mn_{1/3}Nb_{2/3})O_3$ doped PZT.[16] In the literature,[5] the remanent polarization and coercive field with fully saturated loops measured between −200 °C and −70 °C ranged from 5 $\mu C/cm^2$ at 55 kV/cm to 1 $\mu C/cm^2$ at 50 kV/cm, respectively. Taking this into account, together with all of the above mentioned methods of increasing remanent polarization, the estimated values for remanent polarization and coercive field with fully saturated loops of the presented composition were about 4–5 $\mu C/cm^2$ and 25–30 kV/cm, respectively.

Figure 3 shows the measured pyroelectric current of the composition II ceramics generated from temperature fluctuation in the range of 27 to 28.4 °C. The reversed connection made values and polarities of the measured currents completely inverted compared to those of the forward connection, indicating a real pyroelectric response. The pyroelectric coefficient (γ) calculated from the pyroelectric current was 26 $\mu C/m^2 K$. This value is smaller than those of pure KN (93 $\mu C/m^2 K$)[14] and conventional pyroelectric materials.[19] However, it is comparable to that of a ferroelectric polymer, Polyvinylidene fluoride (PVDF, 33 $\mu C/m^2 K$),[20] and larger than that of AlN (6–8 $\mu C/m^2 K$)[21] and ZnO (9.4 $\mu C/m^2 K$).[19] Composition I samples showed 33% smaller γ than the composition II samples. This is expected due to the excessive K^+ vacancies present in composition II, compared to those of composition I, compensating the oxygen vacancies to some extent, thus making the domain wall pinning caused by oxygen vacancies to be less effective.[16,22] Therefore, the polarization could change more easily with temperature than in the case of composition I.

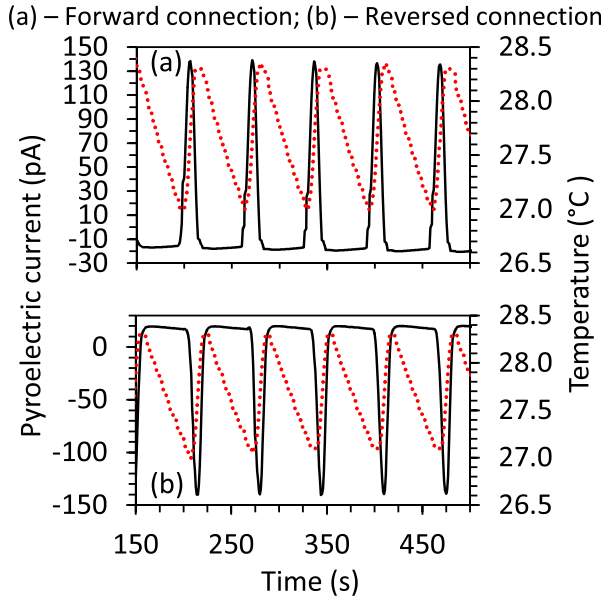

FIG. 3. Pyroelectric current and temperature as a function of time measured with forward and reversed connections for composition II ceramics.

In addition, the composition II samples exhibited d_{33} and g_{33} of 23 pm/V and 4.1×10^{-3} V m/N, respectively. The d_{33} values are comparable to those of PVDF and are larger than those of AlN and ZnO.[23] Although conventional piezoelectrics typically have much larger d_{33}[14,23,24] and PVDF has also been able to simultaneously harvest kinetic and thermal energies,[3] their bandgaps are far away from the range of 1.1–1.5 eV within which the maximum solar energy conversion efficiency has been considered to be achievable.[5,23,25] It should be noted that the individual parameters were not higher than those of optimized ferroelectric or photovoltaic materials in one or two energy regimes. However, the importance of the presented composition lies in the fact that it enables pyroelectric, piezoelectric, and photovoltaic functions simultaneously on a single piece of material. It is expected that with further compositional optimization, the properties will be improved and be more balanced and thus will become more useful for multi-functional purposes.

In summary, 0.1KBNNO ceramics with both a standard stoichiometry and with a modified K-to-Nb ratio have been fabricated and characterized in terms of their ferroelectric, pyroelectric, and piezoelectric properties. The samples have been found to exhibit better pyroelectric and piezoelectric coefficients than ZnO and AlN, which could also be used for harvesting and detecting solar, kinetic, and thermal energies/signals. Meanwhile, as the bandgap of 0.1KBNNO is more feasible for visible light energy conversion than that of the parental composition, it may be considered a proper and capable candidate to trigger developments of all-in-one hybrid energy harvesting and multi-functional sensing devices based on only a single piece of material. Further compositional optimization and device fabrication are on-going.

This work received funding from the European Union's Horizon 2020 research and innovation program under the Marie Sklodowska-Curie Grant Agreement No. "705437." Authors J.P. and J.J. acknowledge the funding from the Academy of Finland (Project Nos. 267573, 273663, and 298409). Author T.S. acknowledges the Riitta, J. J. Takanen, T. Tönning, U. Tuominen, the KAUTE, and Emil Aaltonen Foundations and the Infotech Oulu doctoral program for financial support.

[1]C. Xu, X. D. Wang, and Z. L. Wang, J. Am. Chem. Soc. **131**(16), 5866 (2009).
[2]C. Xu and Z. L. Wang, Adv. Mater. **23**(7), 873 (2011).
[3]Y. Yang, H. L. Zhang, G. Zhu, S. Lee, Z. H. Lin, and Z. L. Wang, ACS Nano **7**(1), 785 (2013).
[4]B. Yang, C. Lee, W. L. Kee, and S. P. Lim, J. Micro-Nanolithogr., MEMS MOEMS **9**(2), 023002 (2010).
[5]I. Grinberg, D. V. West, M. Torres, G. Y. Gou, D. M. Stein, L. Y. Wu, G. N. Chen, E. M. Gallo, A. R. Akbashev, P. K. Davies, J. E. Spanier, and A. M. Rappe, Nature **503**(7477), 509 (2013).
[6]F. Wang and A. M. Rappe, Phys. Rev. B **91**(16), 165124 (2015).
[7]W. Zhou, H. Deng, P. Yang, and J. Chu, Appl. Phys. Lett. **105**(11), 111904 (2014).
[8]U. Fluckiger, H. Arend, and H. R. Oswald, Am. Ceram. Soc. Bull. **56**(6), 575 (1977).
[9]K. Reuter and M. Scheffler, Phys. Rev. Lett. **90**(4), 046103 (2003).
[10]S. J. Zhang, J. B. Lim, H. J. Lee, and T. R. Shrout, IEEE Trans. Ultrason. Ferroelectr. Freq. Control **56**(8), 1523 (2009).
[11]R. G. Sabat, B. K. Mukherjee, W. Ren, and G. Yang, J. Appl. Phys. **101**(6), 064111 (2007).
[12]I. Banik, J. Lukovicova, G. Pavlendova, and R. Podoba, paper presented at the 12th TIM Physics Conference of the West-University-of-Timisoara, Timisoara, Romania, 2012.
[13]R. Lopez and R. Gomez, J. Sol-Gel Sci. Technol. **61**(1), 1 (2012).
[14]H. Birol, D. Damjanovic, and N. Setter, J. Am. Ceram. Soc. **88**(7), 1754 (2005).
[15]J. F. Scott and M. Dawber, Appl. Phys. Lett. **76**(25), 3801 (2000).
[16]B. S. Li, G. R. Li, Q. R. Yin, Z. G. Zhu, A. L. Ding, and W. W. Cao, J. Phys. D: Appl. Phys. **38**(8), 1107 (2005).
[17]M. Kohli, P. Muralt, and N. Setter, Appl. Phys. Lett. **72**(24), 3217 (1998).
[18]T. Rojac, M. Kosec, B. Budic, N. Setter, and D. Damjanovic, J. Appl. Phys. **108**(7), 074107 (2010).
[19]S. B. Lang, Phys. Today **58**(8), 31 (2005).
[20]G. Sebald, D. Guyomar, and A. Agbossou, Smart Mater. Struct. **18**(12), 125006 (2009).
[21]V. Fuflyigin, E. Salley, A. Osinsky, and P. Norris, Appl. Phys. Lett. **77**(19), 3075 (2000).
[22]R. B. Atkin and R. M. Fulrath, J. Am. Ceram. Soc. **54**(5), 265 (1971).
[23]C. R. Bowen, H. A. Kim, P. M. Weaver, and S. Dunn, Energy Environ. Sci. **7**(1), 25 (2014).
[24]H. Birol, D. Damjanovic, and N. Setter, J. Eur. Ceram. Soc. **26**(6), 861 (2006).
[25]A. Niv, Z. R. Abrams, M. Gharghi, C. Gladden, and X. Zhang, Appl. Phys. Lett. **100**(8), 083901 (2012).